Delft University of Technology

FtsZ-Induced Shape Transformation of Coacervates

Fanalista, Federico; Deshpande, Siddharth; Lau, Anson; Pawlik, Grzegorz; Dekker, Cees

Important note
To cite this publication, please use the final published version (if applicable).
Please check the document version above.

FtsZ-induced Shape Transformation of Coacervates

Federico Fanalista[1], Siddharth Deshpande[1], Anson Lau, Grzegorz Pawlik and Cees Dekker[*]

Department of Bionanoscience, Kavli Institute of Nanoscience Delft, Delft University of

Technology, Van der Maasweg 9, 2629 HZ Delft, the Netherlands

[1] Equal contributions

[*]Corresponding author: c.dekker@tudelft.nl

Abstract

Recently, both the cellular and synthetic biology communities have expressed a strong interest in coacervates, membrane-less liquid droplets composed of densely packed multivalent molecules that form as a result of spontaneous phase separation. Here, we study how FtsZ, a protein that plays a key role in the bacterial division process, remodels coacervates made of polylysine (pLL) and guanosine triphosphate (GTP). We show that FtsZ strongly partitions at the surface of the coacervates and induces their disassembly due to the hydrolysis of GTP by FtsZ. Surprisingly, the coacervates are found to promote lateral interactions between FtsZ filaments, inducing the formation of an emanating network of FtsZ bundles that interconnect neighboring coacervates. Under mechanical stress, coacervates are shown to fracture, resulting in profound invaginations along their circumference. Our results bring out the potential of coacervates for their use as membrane-free scaffolds for building synthetic cells as well as are possibly relevant for coacervation in prokaryotic cells.

Introduction

The compartmentalization of biomolecules and regulation of their biological activities are vital aspects of living systems. In order to obtain spatiotemporal control over the numerous chemical reactions occurring within the cell, eukaryotic cells employ internal compartmentalization in the form of membrane-bound organelles. However, it is becoming clear that intracellular organization is not just limited to lipid-encompassed compartments, but is complemented by a variety of membrane-less organelles such as germ granules, stress granules, the nucleolus, and many others.[1] These structures are now being categorized as 'biological condensates', which arise from a physical process of liquid-liquid phase separation, commonly known as coacervation.[2] Coacervation is generally mediated by electrostatic interactions between multivalent molecules, such as polypeptides and nucleotides,[3] where for a certain range of concentrations of such charged molecular species, the decrease in the overall entropy is overcome by the favorable mutual electrostatic attractions, leading to the spontaneous phase separation into a large-volume dilute phase and a small-volume concentrated phase[4]. Importantly, the chemical potentials of the molecular species remain the same in both the phases, thus allowing equilibrium. Owing to the absence of a physical boundary at the interface, such condensates allow for a continuous influx and efflux of individual molecules. Coacervates provide a crowded microenvironment to perform reactions at enhanced rates, they sequester specific molecules promoting their interactions, and they also act as organizing centers.[2] These characteristics of biological condensates make them versatile players in cells. Due to their unique properties, coacervates also provide ample opportunities outside the *in vivo* context of live cells, for example as potential architectural scaffolds for assembling an artificial minimal cell, as an alternative to traditional membranous structures such as liposomes.[5,6]

Given their emerging importance in living cells as well as for in vitro bottom-up biology, various aspects of coacervates are currently being studied extensively, for example how external parameters (pH and ionic strength), as well as the properties of the coacervate components (molecular length and charge content), affect the formation and dissolution of polypeptide-based coacervates.[7] Also, the manipulation of coacervates has been explored using enzymatic reactions that

enhance/decrease the multivalent nature of specific components.[8,9] Interestingly, various cytoskeletal proteins such as actin and microtubules were shown to partition into coacervates, resulting in an enhanced activity and even significant changes of the coacervate morphology.[10,11]

While the majority of these studies involved proteins belonging to eukaryotic systems, the same principles may apply to prokaryotic biomolecules such as FtsZ, a central protein essential for the process of cell division in most bacteria.[12] As a prokaryotic homologue of tubulin,[13] FtsZ polymerizes into filaments that assemble into a ring structure at the cell mid-plane. This structure serves as a scaffold to recruit and coordinate further proteins constituting the so-called Z-ring,[14] which directs the constriction and division of the cell into two daughters. Guanosine triphosphate (GTP) plays a fundamental role in the assembly[15] and dynamics of FtsZ filaments. Two FtsZ monomers can stably bind by incorporating a GTP molecule at their interface, and repetition of such dimerization leads to the assembly of ~100 nm long filaments.[16] The GTP is hydrolyzed into GDP (guanosine diphosphate) with a rate that strongly depends on the buffer conditions.[17] As the GTP gets hydrolyzed by FtsZ, the bond between two FtsZ monomers gets weaker and prone to unbinding. The process of continuous GTP hydrolysis and repletion leads to the turnover of monomers and filament treadmilling dynamics, as has been shown *in vitro*[18] as well as in vivo. The recent discovery of the treadmilling dynamics *in vivo* indicated that FtsZ is the main architectural driver for the synthesis of new cell wall.[19] *In vitro* reconstitutions of FtsZ filaments inside liposomes has shown how the protein on itself is capable to deform the lipid membrane,[20,21] suggesting the possibility to employ the protein to re-create a minimal artificial divisome. A popular model for force generation by FtsZ is based on the higher curvature of GDP-bound FtsZ filaments compared to GTP ones,[22] suggesting GTP hydrolysis as the energy source for bending force. *In vitro* reconstitution of FtsZ inside liposomes has also shown that FtsZ bundles can deform the soft membrane with dynamics that depend on the GTP hydrolysis rate.[23] In comparison, the possibility of FtsZ to interact with membrane-less coacervates is largely unexplored. A recent *in vitro* work has shown that FtsZ forms coacervates with SlmA,[24] a protein involved in the inhibition of the septal ring assembly in the vicinity of chromosomes. However, it remains to be seen whether FtsZ has the ability to dynamically interact with membrane-less

condensates, possibly leading to morphological changes to them, as is the case with membrane-bound containers.

In this paper, we use a microfluidic set up to study the dynamics of a three-component system: FtsZ, the key protein involved in bacterial division; polylysine (pLL) which is a positively charged multivalent peptide; and GTP as a negatively charged multivalent nucleoside triphosphate. While pLL and GTP self-assemble to form coacervates, FtsZ is a GTPase and thus has the potential to impact the stability of these coacervates. We show that FtsZ filaments partition strongly at the interface of pLL-GTP coacervates where they can induce a variety of morphological changes. Under continuous flow of a buffer without GTP, we observe an isotropic shrinkage of coacervates, which can be attributed to the hydrolysis of GTP molecules by FtsZ. Indeed, externally providing GTP to compensate for its loss from the condensate prevents any structural changes to the coacervates. Furthermore, we observe that FtsZ filaments assemble into thick bundles at the coacervate interface. Such bundling is remarkable, as it is observed in vitro only in the presence of crowding agents[25] or additional accessory proteins that *in vivo* form crosslinks between the FtsZ filaments.[26][27] Interestingly, these bundles do not remain confined to the interface, but grow and emanate from the coacervates, ultimately joining each other to form a dense network of bundles. Lastly, compressing the FtsZ-coated coacervates causes them to fracture, leading to distinct flower shapes with pronounced indentations.

By selecting a key bacterial divisome protein and using the energy source for its polymerization as one of the components of the coacervate, we thus are able to observe interesting morphological changes of the coacervate itself. In the context of assembling a minimal divisome, the basic requirements of a minimal scaffold for an artificial cell include the need to induce localization of the proteins, to preserve and enhance their functionality, to allow energy exchange, and to undergo morphological changes. The remarkable partitioning of FtsZ on the surface of coacervates in the absence of a lipid membrane, the enhanced assembling into bundles without additional promoters, and the ability of FtsZ to induce morphological changes to the coacervates, are encouraging indicators that coacervates may indeed constitute a membrane-free alternative scaffold for minimal artificial cells. The observed phenomena may also have biological relevance for the localization and bundling of FtsZ filaments *in vivo,* suggesting that coacervation may also be a relevant feature in prokaryotic cells.

Materials and Methods

Microfabrication and soft lithography

Microchamber designs were produced in a cleanroom with the following procedure: a 4 inch silicon wafer was cleaned in fuming nitric acid (100% HNO_3) for 10 minutes using a sonication bath, and further rinsed with water. The wafer was then spin-coated with hexamethyldisilazane (HMDS) and subsequently with NEB22a (Sumitomo Chemical) negative resist. Both layers were spun at 1000 rpm for 1 minute and baked at 200 °C for 2 minutes and 110 °C for 3 minutes respectively. The HMDS layer is necessary to ensure proper adhesion of NEB22a onto the silicon surface. Electron-beam lithography (EBPG-5000+, Raith GmbH) was used to write the designs on the coated wafer (dose: 16 µC cm^{-2}, acceleration voltage: 100 kV, aperture: 400 µm). A post-bake was performed at 105 °C for 3 minutes. The structures were developed in MF322 (Dow Chemical Company) for 30 seconds, followed by rinsing in diluted MF322 (10 times in deionized water) for 15 seconds, and finally rinsing in deionized water for 15 seconds. Structures were then dry-etched using Bosch deep reactive-ion etching, with an inductive coupled plasma (ICP) reactive-ion etcher (Adixen AMS 100 I-speeder). The procedure consisted of alternating SF_6 etching steps with C_4F_8 passivation steps. At the end of the process, the wafer was exposed to Oxygen plasma for 10 minutes to remove the excess of resist from the wafer. To facilitate subsequent peeling-off of polydimethylsiloxane (PDMS) from the wafer, the hydrophobicity of the surface was enhanced by silanizing it with (tridecafluoro-1,1,2,2-tetrahydrooctyl) trichlorosilane (ABCR GmbH & Co.) overnight in a vacuum desiccator.

Curing agent and PDMS (Mavom) were mixed in a mass ratio 1:10, degassed in vacuum, and the mixture was poured on a plain silanized wafer and on the wafer containing the required patterns. The plain wafer was used to prepare glass coverslips with a thin PDMS coating. For that, coverslips were firmly pressed down on the wafer, so that a thin PDMS layer was formed beneath them. Both wafers were baked at 80 °C for 4 hours. Coverslips and the PDMS block containing the designs were removed from the wafers, and single microchambers were separated with a cutter and cleaned using isopropanol. Both chips and coverslips were activated using Oxygen plasma

(Plasmatic System, Inc.) for about 10 seconds, then immediately bonded and baked for other 20 minutes at 80 °C.

The solutions were introduced into the microchambers using pressure pumps (Fluigent) via appropriately connected tubing (Tygon Microbore Tubing, inner diameter) and home-built metal connectors. The flow was finely tuned using a MAESFLO software (Fluigent).

Wedge device preparation

A piece of double-face Scotch tape was put at one end of a coverslip, along with 40 μl of sample. A second coverslip was then put on top, with one end in contact with the bottom coverslip and the other end on the tape, to create the desired tilted angle. Finally, the sides of the resulting wedge geometry were sealed with epoxy (Devcon). Before preparing the device, the coverslips were surface covered with fluorescent labels in order to precisely measure the height throughout the device. For labeling the surfaces, a drop of a solution containing cy5-labeled MinE protein (1 μM) was squeezed between two PDMS-covered coverslips. After incubating for 30 minutes, the coverslips were extensively washed with MilliQ water to remove the excess of proteins from the surface.

Coacervates preparation

Unlabeled polylysine (15-30 kDa) was purchased from Sigma Aldrich. Polylysine (~25 kDa), labeled with cy5 fluorescent dye, was purchased from Nanocs. The powders were dissolved in MilliQ water at a concentration of 50 mg/mL and 1mg/mL, respectively. Labeled and unlabeled polylysine were mixed together in a molar ratio of 1:100. Guanosine triphosphate sodium salt hydrate was purchased from Sigma Aldrich and dissolved in MilliQ water to a final stock concentration of 100 mM. Just before the experiment, GTP and pLL were diluted separately to 25 mM and 0.44 mM respectively. Finally, 20 μl of solution containing 25 mM GTP was mixed with 20 μl solution containing 0.44 mM pLL by pipetting up and down extensively. Guanosine diphosphate sodium salt was purchased from Sigma Aldrich. Preparation of stock solutions and coacervates with GDP followed the same procedure as described for GTP.

Solution compositions

The composition of the aqueous solution containing FtsZ was as follows: 12 μM FtsZ, 180 mM KCl, 25 mM Tris-HCl (pH 7.4), 5 mM MgCl$_2$, 15% v/v glycerol. When required, 25 mM GTP was added to the solution. The aqueous solution used to remove excess of proteins and nucleotides from the microchamber had the following composition: 150 mM KCl, 25 mM Tris HCl (pH 7.4), 5 mM MgCl$_2$. Again, if the experiment required it, 25 mM GTP was added. FtsZ purification and labeling (with Alexa Fluor 488) were performed in the lab following the protocol described elsewhere.[28] Protein plasmids were a kind gift from Germán Rivas (Centro de Investigaciones Biológica-CSIC, Madrid). Labeled and unlabeled FtsZ were mixed in a ratio 1:8, flash-frozen in liquid nitrogen and stored at -80 °C.

Image acquisition and processing

Sample imaging was performed using an Olympus IX-81 inverted microscope with epifluorescence illumination and specific filter sets. Images were acquired using 20x UPlanSApo (NA 0.75) and 60x PlanApo (NA 1.45, oil) objectives, and recorded with a Zyla 4.2 PLUS CMOS camera (Andor Technology) and a micromanager software (version 1.4.14). Confocal imaging was performed using an inverted Olympus IX81 combined with Andor Revolution illumination system. Confocal images were acquired using a Yokogawa CSU X1 detection system, a 60x UPlanFLN (NA 1.25) objective, and an EM-CCD Andor iXon X3 DU897 camera. Images were analyzed and background appropriately subtracted using Fiji (ImageJ).

Zeta potential measurements

For zeta potential measurements (Zetasizer Nano, Malvern Instruments), pLL/GTP coacervates were prepared by mixing 20 uL of 0.44 mM (15-30 kDa) pLL and 20 uL of 25 mM GTP, and vortexing for 10 seconds. 10 uL of the resulting solution was immediately taken and diluted in 760 uL of MQ water and equilibrated for 2 hours before inserting it into a flow cell. For measurements involving FtsZ-coated coacervates, 20 uL of unlabeled FtsZ solution in buffer was added to the coacervates and mixed by pipetting up and down. The rest of the procedure was as described above.

Statistical analysis

The size distribution of the coacervates (Fig. S1) was obtained by manually measuring the diameter of individual coacervates (n = 331). The diameter of flower-shaped coacervates was determined similarly (Fig. 4c). The diameter values were acquired for 540 coacervates, of which 70 showed clear fracturing. The local height of the wedge-shaped device was measured by taking a stack of images (step = 1 µm) along the z-axis of the device and further measuring the distance between the two fluorescent peaks, corresponding to the two labeled coverslips.

To calculate the partition coefficients, a fluorescent intensity profile for each coacervate (n = 24) was obtained along the equatorial plane. The fluorescence at the surface was determined as the peak of the intensity profile, while the intensity inside and outside the coacervates was determined as the lowest values in their respective regions.

The error bars in all of the analyses correspond to a single standard deviation. All of the image processing was done using Fiji (ImageJ) and the graphs were plotted using MATLAB 2015 (Mathworks).

Results

FtsZ partitions at the interface of GTP/pLL coacervates

Coacervation of pLL and GTP took place readily, and could be seen by the immediate increase in the turbidity of the solution. To maximize the size of the coacervates and minimize the free charges in the diluted phase to a negligible amount, we mixed pLL and GTP in a stochiometric ratio such as to balance their negative and positive charges (see Materials and Methods). The obtained coacervates were flushed into a PDMS-based microchamber, where they sedimented and adhered to the bottom of the chamber. This adherence helped the coacervates maintain their position despite a flow, allowing stable imaging over long times during experimentation. Coacervates that were still floating in the microchamber merged with the adhered ones, forming bigger coacervates, resulting in polydispersely sized samples (Fig. S1). This process of coalescences was continued until a sizeable fraction of coacervates reached a diameter $d \geq 5$ µm, a size convenient for visualization (Fig. 1a). As expected, the fluorescent signal from pLL was homogeneously distributed in the coacervates (Fig. 1b).

To examine how FtsZ interacted with the pLL/GTP coacervates, a solution containing FtsZ and GTP was flushed in the microchamber. We observed immediate, pronounced localization of FtsZ at the interface of the coacervates, in the form of a bright fluorescent ring at the equatorial plane (Fig. 1c). To analyze the preferential localization of FtsZ at the interface between the two liquid phases, we compared the fluorescent signal in the interior and at the interface of the coacervates with that measured in the surrounding dilute phase. When the coacervates and the FtsZ solution were simply mixed in equal amounts, we obtained an internal partition coefficient $P_i=0.6\pm0.1$ (mean ± standard deviation) and a surface partition coefficient $P_s=2.3\pm0.3$ ($n=30$). On the other hand, when we constantly flushed FtsZ solution through the chamber, we observed an increase in the magnitude of the surface partition coefficient. After one hour of constant flushing, we measured $P_i= 0.7\pm0.2$ and $P_s=4.5\pm1.2$ ($n_s=24$), indicating that the fraction of proteins partitioned on the surface of the coacervates increased as more proteins were provided via the surrounding solution. The internal partition coefficient, on the other hand, remained unchanged.

The reason for the preferential localization of FtsZ on the surface of the coacervates is likely the electrostatic interactions between the FtsZ protein filaments and the coacervates. To understand the process, we measured the zeta potential relative to the surface of GTP/pLL coacervates. In the absence of FtsZ, we obtained a value Z=12.7±2.3 mV (n_{runs}=6) indicating that the interface was positively charged, likely due to an excess of pLL molecules on the surface of coacervates. Since FtsZ is overall negatively charged at pH 7.4 (given its isoelectric point of 4.9[29]), it will be driven to the surface through electrostatic attraction. Indeed, when we measured the Z potential on FtsZ-coated coacervates, we obtained Z=-5.8±0.6 mV (n_{runs}=12), consistent with the fact that the negatively charged FtsZ molecules were covering the coacervates.

GTP hydrolysis by FtsZ induces disassembly of coacervates

Realizing the strong tendency of FtsZ to concentrate on the surface of the coacervates, we wondered whether the GTPase activity of FtsZ could induce morphological changes to the liquid droplets. As stability of coacervates critically relies on the balanced interaction between opposite charges, hydrolysis of GTP to GDP and a phosphate group, which reduces the number of negative charges per molecule, would be expected to destabilize the liquid droplets.

Indeed, we observed that GTP hydrolysis by FtsZ significantly affects the coacervates. This is illustrated in Fig. 2a, where we flushed the coacervates with a solution containing FtsZ and GTP, followed by a buffer solution to remove the excess of proteins and nucleotides from the microchamber: after the first 5 minutes, the FtsZ fluorescent signal started to become more homogenous over the coacervates. This was probably due to a continuous reduction of the coacervate volume, with the top surface now coming into the initial equatorial focal plane. After 20 minutes, the reduction of the volume became much more pronounced, as the coacervates dramatically shrunk to less than half of their original diameter. The FtsZ shell around the coacervates concomitantly decreased in diameter, with FtsZ following the shrinking outer contour of the coacervates. Ultimately, the coacervates underwent a drastic reduction in their volume, to the point that only very small agglomerates were left. The overall collapse of the coacervates structure can be attributed to the

hydrolysis of GTP by FtsZ. As the nucleotides get hydrolyzed, the phosphates are prone to leave the coacervates, creating a deficiency of negative charges. As a result, excess pLL gets released in the surrounding solution together with GDP, as schematically shown in Fig. 2c. This explains the continuous shrinkage of the coacervates. The resulting remnants might be made up of some pLL and FtsZ residuals adhering together, or they could be pLL/GDP coacervates still covered by a layer of FtsZ. In the latter case, the smaller coacervate size can be given by the fact that GDP, having less charges than GTP, leads to a less efficient coacervation. To explore this possibility, we formed coacervates by mixing GDP and pLL in the same stoichiometric ratio as the one used for GTP/PLL coacervates (Fig. S2). In these conditions, we indeed observed negligible amount of coacervation; only a few very small droplets were visible.

To verify that the observed shrinkage is indeed a consequence of the GTPase activity of FtsZ, we investigated whether the coacervates were able to replace any hydrolyzed GTP by the uptake of fresh GTP molecules from the surrounding environment and thus prevent their disassembly. Indeed, in conditions where we flushed a solution containing GTP through the chamber, the coacervates remained stable and their size remained unchanged over time (Fig. 2b). It appears that in this case, the efflux of GDP generated by hydrolysis of GTP in the coacervates was compensated by an influx of fresh GTP, as schematically shown in Fig. 2d. This maintained the charge balance and hence the structural stability. Finally, when we repeated the experiment illustrated in Fig. 2a in absence of FtsZ, the coacervates did not show any appreciable change in size, further confirming that the observed shrinkage is indeed a consequence of the FtsZ activity (Fig. S3). Thus, we conclude that pLL/GTP coacervates not only serve as energy reservoir by providing GTP to the adhered FtsZ, but they can also replenish the energy-rich molecules from the surrounding environment.

Localization on the coacervate surface promotes bundling of FtsZ filaments

Together with the capability of FtsZ to reshape GTP/pLL coacervates, we observed that the coacervates promoted the aggregation of FtsZ filaments into a dense interconnected network of bundles, which we were able to visualize using confocal microscopy (Fig. 3a). We flushed a solution containing FtsZ and GTP in a microchamber containing GTP/pLL coacervates for about two hours, instead of twenty minutes as with previous experiments, in order to increase the FtsZ concentration on the coacervate surface and promote bundle formation. In order to visualize the possible microstructures, we removed the excess of proteins from the microchamber by gently flushing a protein-free buffer solution, until the fluorescent background was greatly reduced.

Interestingly, we observed a network of filamentous structures protruding from the coacervates into the surrounding environment, so that the coacervates appeared like aster-like objects. We measured the distribution of FtsZ in different planes along the *z*-axis (Fig. 3b). At the top surface of the coacervates, FtsZ filaments had clearly reorganized in filamentous bundles. At the equatorial plane, localization of FtsZ filaments on the surface was evident, as well as the bundles emerging out of the surface. Interestingly, in absence of a physical membrane and membrane-anchoring proteins such as ZipA and FtsA, FtsZ bundles did not remain confined at the interface, but grew out into the surrounding environment. At the bottom plane, the contact surface between the PDMS and the coacervate was free of proteins and appeared as dark disk, and it was surrounded by an interconnected network of FtsZ bundles emanating from neighboring coacervates.

If the gentle buffer flow was continued, the coacervates underwent the same shrinkage process as previously described (Fig. 2a). However, a dense network of thick bundles surrounding the small shrunken agglomerates remained present towards the sides of the microchamber, where the flow was relatively weak and thus did not disrupt the network of bundles. Interestingly, the long filamentous structures constituting this network were composed of both FtsZ and pLL (Fig. S4). As the FtsZ bundles protruded out of the coacervates, the pLL molecules thus appeared to interact and co-localize with them.

To better assess the reason behind the enhanced bundling of FtsZ, we looked at the interaction between pLL and FtsZ, in absence of GTP. It was evident that, even in absence of coacervation, pLL and FtsZ still interacted to form fiber-like structures (Fig. S5). Even if these filamentous assemblies looked different from the FtsZ bundles obtained in presence of coacervates (Fig. 3 and Fig. S4), it seems reasonable to attribute the enhanced bundling properties of FtsZ to the presence of positive charges carried by pLL on the coacervate surface. Possibly, pLL acts as a bundling agent and through counterion condensation, promotes the lateral association of negatively charged FtsZ filaments into bundles.

Coacervates 'crack' and develop invaginations under mechanical stress

Finally, we investigated whether the localization of FtsZ at the interface of the coacervates influences their mechanical properties. To check how the coacervates react under mechanical stress, we squeezed ~20 μL solution containing FtsZ and pLL/GTP coacervates between two coverslips. To our surprise, the bigger coacervates seemed to 'crack open' and showed deep invaginations, giving them a flower-like appearance. The number of invaginations tended to increase with the coacervate size and their location was fairly evenly placed along the circumference. These flowers sometimes displayed prominent triangular petals, seemingly on the verge of separation from each other (Fig. 4a). The coacervates thus appeared to behave more like gel/glass-like objects than like liquid droplets, as upon pressing the sides of the droplets, where the stress tensor was highest, ripped apart to form a flower-like shape. To check whether this effect was indeed caused by the mechanical stress applied on the coacervates, we employed a wedge device (Fig. 4b), where the distance h between the two coverslips was varied from tens of micrometers to less than a micrometer. By having the two coverslips fluorescently labeled, it was possible to measure h for each field-of-view and compare it with the diameter d of the coacervates. By comparing h and d, we could infer whether each coacervate was vertically confined ($h/d<1$) or not ($h/d>1$). Plotting a frequency histogram of 'flowers' and regular spheres against h/d (Fig. 4c) showed that the flower shape was exclusively obtained for $h/d <1$, showing that, indeed, the flowers were induced by the mechanical stress applied on the coacervates.

Several control experiments were performed to check whether this effect was indeed given by the presence of FtsZ and its activity on the surface of the coacervates. Compressing pure coacervates in absence of FtsZ did not lead to any deformations, and the coacervates behaved like liquid droplets (Fig. S6a). Repeating the mechanical test on ATP/pLL coacervates mixed with FtsZ solution also resulted in liquid droplets without any deformations (Fig. S6b). However, when we mixed GTP/pLL coacervates with just the buffer that FtsZ was dissolved in, we again observed flower-like deformations, although to a lesser extent and less symmetric than those seen in presence of FtsZ (Fig. S6c). Possibly, the presence of FtsZ filaments and their interaction with pLL created a relatively rigid layer around the coacervate, producing deeper and more regular fractures under mechanical stress. Even more surprisingly, when we performed the previous experiment with ATP/pLL coacervates, we did not observe these fractures. This led us to conclude that the 'flower formation' is dependent on the specific nucleotide (GTP against ATP) used to form the coacervates. When glycerol was removed from the buffer to check the effect of viscosity, the flower shape remained absent (Fig. S6e), and also when all the individual components of the buffer were mixed separately with GTP/pLL coacervates (Fig. S6f-i). Thus, the severe shape deformations of FtsZ-coated coacervates under mechanical stress that we observe may not be solely induced by FtsZ, but instead, they are more likely enhanced by its presence at the interface.

On the dependence of the specific nucleotide, we note that it is plausible that, given the different molecular structure of their bases, GTP molecules form more extensive hydrogen bonding with polylysine polymers as compared to ATP molecules, creating more compact, and hence less deformable, coacervates. Also, the presence of cations, such as K^+, has been reported to enhance the formation of hydrogen bonds between the guanine bases.[30] Furthermore, π-π stacking of the aromatic surfaces can lead to the creation of supramolecular assemblies inside the coacervates,[31] potentially transforming the droplets from a liquid phase into a denser gel phase.

Discussion

In this work, we explored how FtsZ, a highly conserved protein responsible for cell division in bacteria, dynamically interacts with liquid droplets (coacervates) made up of polylysine and GTP. By performing microfluidic on-chip experiments, we showed that FtsZ partitions at the coacervate interface where it is able to induce structural changes and reshape the coacervates. At the same time, the liquid droplets also have a clear impact on the self-assembly of FtsZ filaments. Our data shows that, despite the lack of a lipid membrane and membrane-anchoring proteins, FtsZ strongly localizes at the surface of the coacervates. Due its GTPase nature, FtsZ further utilizes the high concentration of GTP within the droplets as an energy reservoir, which destabilizes the coacervates and induces their disassembly. When GTP is externally provided, the shrinkage process is completely inhibited as the hydrolyzed GTP is continuously replenished.

Another key feature of FtsZ filaments that we have observed is their lateral organization into bundles in absence of any external agent. In bacteria, FtsZ filaments laterally associate into bundles that further constitute the ring structure responsible for the division. *In vitro*, this self-assembly process can occur in confined environments in the presence of additional macromolecules such as Ficoll or polyethylene glycol, that recreate the necessary crowding conditions.[25] Other *in vitro* works have shown aggregation of FtsZ filaments into bundles by interaction with specific proteins that play the role of crosslinks between the filaments *in vivo*, such as the membrane anchor ZipA[27] or the bundling agent ZapA.[32] Finally, FtsZ has been reported to form dynamic bundles when tethered to a lipid membrane via one of its natural anchor proteins,[18] or when modified to bind a lipid membrane without the need of additional proteins.[33]

We showed that the lateral association between FtsZ filaments, when partitioned on the surface of the coacervates, enriched of the positively charged pLL molecules, is enhanced. The consequent bundling of FtsZ filaments constitutes a mode of spatial organization that doesn't involve auxiliary crowders or proteins that are normally required for FtsZ to bundle *in vitro* and *in vivo*. The bundling of FtsZ on the surface induced a morphological change, where the liquid droplets acted as nodes with FtsZ bundles protruding out in the surrounding environment, creating a dense network.

Our results bear some resemblance to a previous report, where the pH-triggered assembly of nanofibers drove spontaneous shape transformation of spherical coacervates into aster-like fibrous structures.[34] Also, shape deformation of coacervates induced by polymerization of tubulin cytoskeletal proteins was recently observed, where the growth of microtubules inside coacervates led to a rod-like shape.[10]

Finally, we observed that FtsZ-coated coacervates, when subjected to mechanical pressure, showed unexpected solid-like behavior, which manifested itself in the form of deep invaginations, giving them a flower-like appearance. Although this effect is more pronounced with protein-coated droplets, we observed similar deformations under specific conditions without any proteins, and the observed intriguing phenomenon can be attributed to the presence of a specific nucleotide in specific buffer conditions.

Overall, we explored the use of coacervates as both potential scaffolds as well as energy reservoirs for NTPase proteins such as FtsZ. We showed how GTP/pLL coacervates provide and exchange nucleotides with the surrounding environment and the proteins. The self-assembly of FtsZ filaments, which were partitioned on the surface of the coacervates, was greatly enhanced and the formed protein bundles reshaped the liquid droplets. Such a dynamic system might prove to be an important tool in synthetic biology, especially towards the creation of a minimal cell. The strong affinity of FtsZ for coacervates may also be of relevance in bacteria where, along with other factors, the localization and bundling of FtsZ filaments at the mid-cell could be facilitated by coacervation.

References

[1]   S. F. Banani, H. O. Lee, A. A. Hyman, M. K. Rosen, *Nat. Rev. Mol. Cell Biol.* **2017**, *18*, 285.

[2]   Y. Shin, C. P. Brangwynne, *Science* **2017**, *357*, DOI 10.1126/science.aaf4382.

[3]   S. Koga, D. S. Williams, A. W. Perriman, S. Mann, *Nat. Chem.* **2011**, *3*, 720.

[4]   A. A. Hyman, C. A. Weber, F. Jülicher, *Annu. Rev. Cell Dev. Biol.* **2014**, *30*, 39.

[5]   W. K. Spoelstra, S. Deshpande, C. Dekker, *Curr. Opin. Biotechnol.* **2018**, *51*, 47.

[6]   M. Li, X. Huang, T. Y. D. Tang, S. Mann, *Curr. Opin. Chem. Biol.* **2014**, *22*, 1.

[7]   D. Priftis, M. Tirrell, *Soft Matter* **2012**, *8*, 9396.

[8]   W. M. Aumiller, C. D. Keating, *Nat. Chem.* **2015**, *8*, 129.

[9]   K. K. Nakashima, J. F. Baaij, E. Spruijt, *Soft Matter* **2017**, DOI 10.1039/C7SM01897E.

[10]   A. Hernández-Vega, M. Braun, L. Scharrel, M. Jahnel, S. Wegmann, B. T. Hyman, S. Alberti, S. Diez, A. A. Hyman, *Cell Rep.* **2017**, *20*, 2304.

[11]   P. M. Mccall, S. Srivastava, S. L. Perry, D. R. Kovar, M. L. Gardel, M. V Tirrell, *bioarxiv* **2017**, DOI 10.1101/152025.

[12]   K. Dai, J. Lutkenhaus, *J Bacteriol* **1991**, *173*, 3500.

[13]   H. P. Erickson, *Cell* **1995**, *80*, 367.

[14]   T. den Blaauwen, L. W. Hamoen, P. A. Levin, *Curr. Opin. Microbiol.* **2017**, *36*, 85.

[15]   A. Mukherjee, J. Lutkenhaus, *EMBO J.* **1998**, *17*, 462.

[16]   Y. Chen, H. P. Erickson, *J. Biol. Chem.* **2005**, *280*, 22549.

[17]   A. Mukherjee, J. Lutkenhaus, *J. Bacteriol.* **1999**, *181*, 823.

[18]   M. Loose, T. J. Mitchison, *Nat. Cell Biol.* **2014**, *16*, 38.

[19]   A. W. Bisson-Filho, Y. P. Hsu, G. R. Squyres, E. Kuru, F. Wu, C. Jukes, Y. Sun, C. Dekker, S. Holden, M. S. VanNieuwenhze, Y. V. Brun, E. C. Garner, *Science* **2017**, *355*, 739.

[20]   P. Szwedziak, Q. Wang, T. A. M. Bharat, M. Tsim, J. Löwe, *Elife* **2014**, *3*, e04601.

[21]   M. Osawa, H. P. Erickson, *Proc. Natl. Acad. Sci. U. S. A.* **2013**, *110*, 11000.

[22]   C. Lu, M. Reedy, H. P. Erickson, *J. Bacteriol.* **2000**, *182*, 164.

[23]   E. J. Cabré, A. Sánchez-Gorostiaga, P. Carrara, N. Ropero, M. Casanova, P. Palacios, P. Stano, M. Jiménez, G. Rivas, M. Vicente, *J. Biol. Chem.* **2013**, *288*, 26625.

[24] B. Monterroso, S. Zorrilla, M. Sobrinos-Sanguino, M. A. Robles-Ramos, M. López-Álvarez, C. D. Keating, G. Rivas, *bioRxiv* **2018**.

[25] J. Groen, D. Foschepoth, E. Te Brinke, A. J. Boersma, H. Imamura, G. Rivas, H. A. Heus, W. T. S. Huck, *J. Am. Chem. Soc.* **2015**, *137*, 13041.

[26] F. J. Gueiros-Filho, R. Losick, *Genes Dev.* **2002**, *16*, 2544.

[27] C. A. Hale, A. C. Rhee, P. A. J. De Boer, A. M. Y. C. Rhee, *Society* **2000**, *182*, 5153.

[28] J. M. González, M. Jiménez, M. Vélez, J. Mingorance, J. M. Andreu, M. Vicente, G. Rivas, *J. Biol. Chem.* **2003**, *278*, 37664.

[29] Q.-M. Yi, J. Lutkenhaus, *Gene* **1985**, *36*, 241.

[30] J. T. Davis, G. P. Spada, *Chem. Soc. Rev.* **2007**, *36*, 296.

[31] S. Lena, S. Masiero, S. Pieraccini, G. P. Spada, *Chem. - A Eur. J.* **2009**, *15*, 7792.

[32] H. H. Low, M. C. Moncrieffe, J. Löwe, *J. Mol. Biol.* **2004**, *341*, 839.

[33] M. Osawa, D. E. Anderson, H. P. Erickson, *Science* **2008**, *320*, 792 LP.

[34] R. Krishna Kumar, R. L. Harniman, A. J. Patil, S. Mann, *Chem. Sci.* **2016**, *7*, 5879.
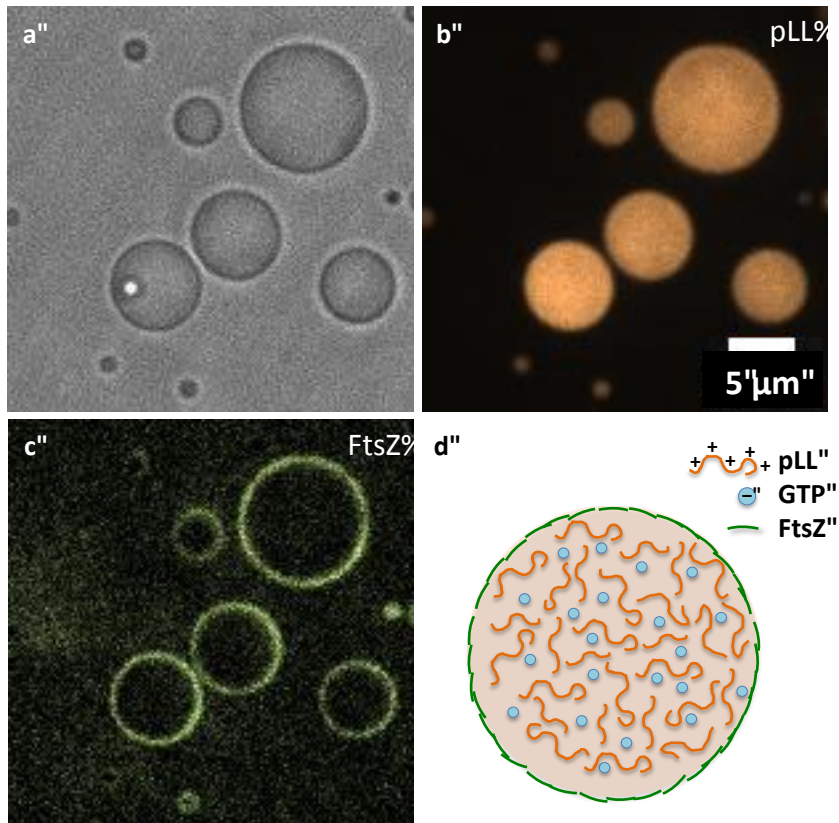
Figure 1. FtsZ localizes at the interface of self-assembled pLL/GTP coacervates.

(**a**) Bright-field image showing a polydisperse population of coacervates in a PDMS-based microchamber. These membrane-less droplets are spontaneously formed as a result of electrostatic interactions between positively charged pLL and negatively charged GTP molecules. (**b**) Fluorescence image (false color) showing that such phase-separated droplets indeed have an increased concentration of pLL inside them. pLL is labeled with cy5 for visualization. (**c**) Fluorescence image (false color) showing that FtsZ strongly partitions at the interface of the coacervates. 11% of the protein molecules were labelled with Alexa Fluor 488 for visualization. (**d**) Schematic representation of pLL/GTP condensates with localization of FtsZ filaments at the interface.
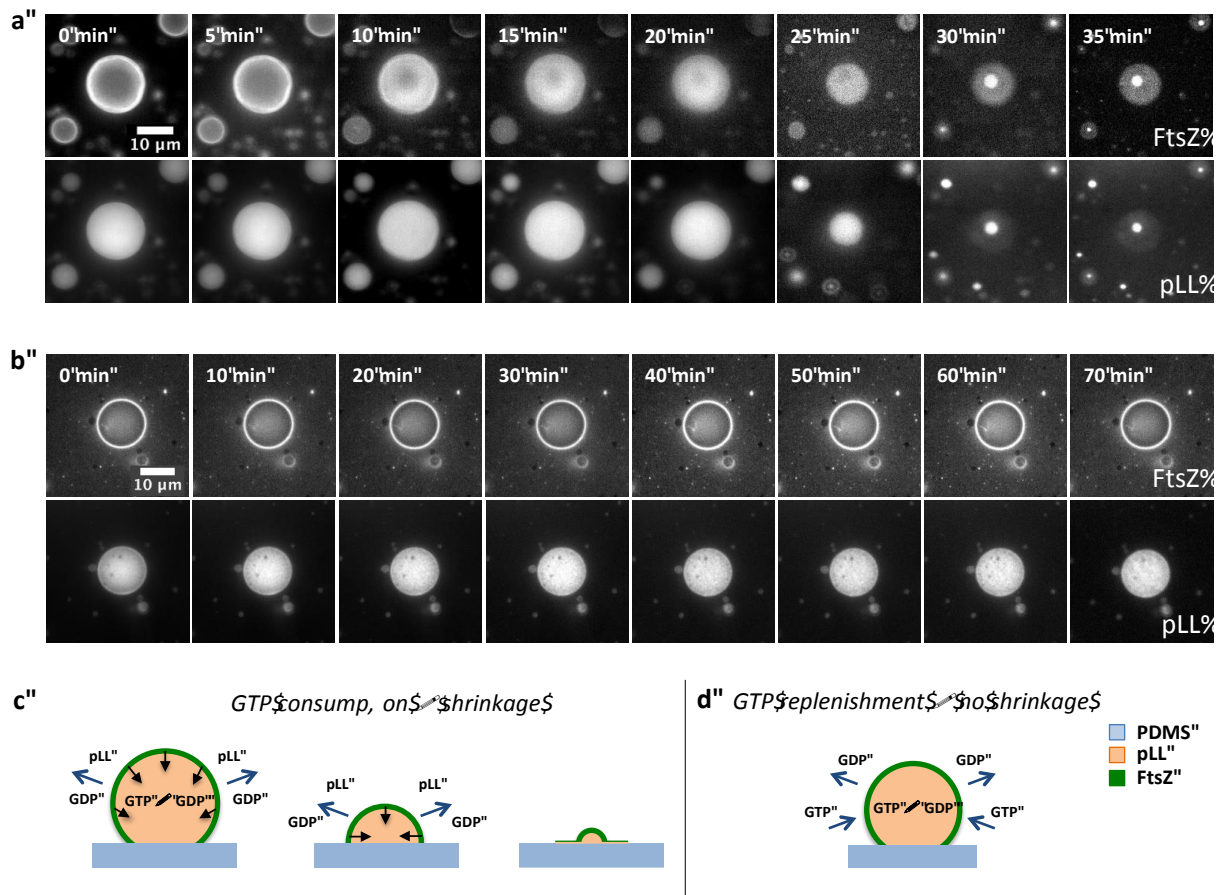
Figure 2. GTP hydrolysis by FtsZ filaments promotes rapid disassembly of coacervates, leading to isotropic shrinkage.

(**a**) Once FtsZ-coated coacervates were washed free of any excess protein and GTP in the surrounding environment, the coacervates became unstable and underwent a drastic shrinkage. The end state showed small bright aggregates, presumably composed of FtsZ and pLL remnants. A faint halo observed around the remnants is probably a mark left from the original contact area between the coacervate and the microchamber. (**b**) Coacervate instability (in the form of shrinkage) is not observed, if GTP is externally provided to replenish the GTP hydrolyzed by FtsZ. The coacervates maintained their shape and size over a prolonged period of time. (**c**) Schematic interpretation of the disassembly process: as FtsZ hydrolyses trivalent GTP molecules into divalent GDP molecules, the balance between positive and negative charges within the coacervates is altered. As this process continues, the electrostatic interactions are weakened and as a result, pLL and GDP molecules are released from the coacervates into the surrounding solution, and the coacervates shrink. d) Schematic interpretation to explain the observed stability of coacervates when GTP is externally provided. The

GTP turnover inside the coacervates is balanced by the influx of GTP. As a result, the coacervates are able to replace the newly formed GDP with GTP to preserve the charge balance and thus their integrity.
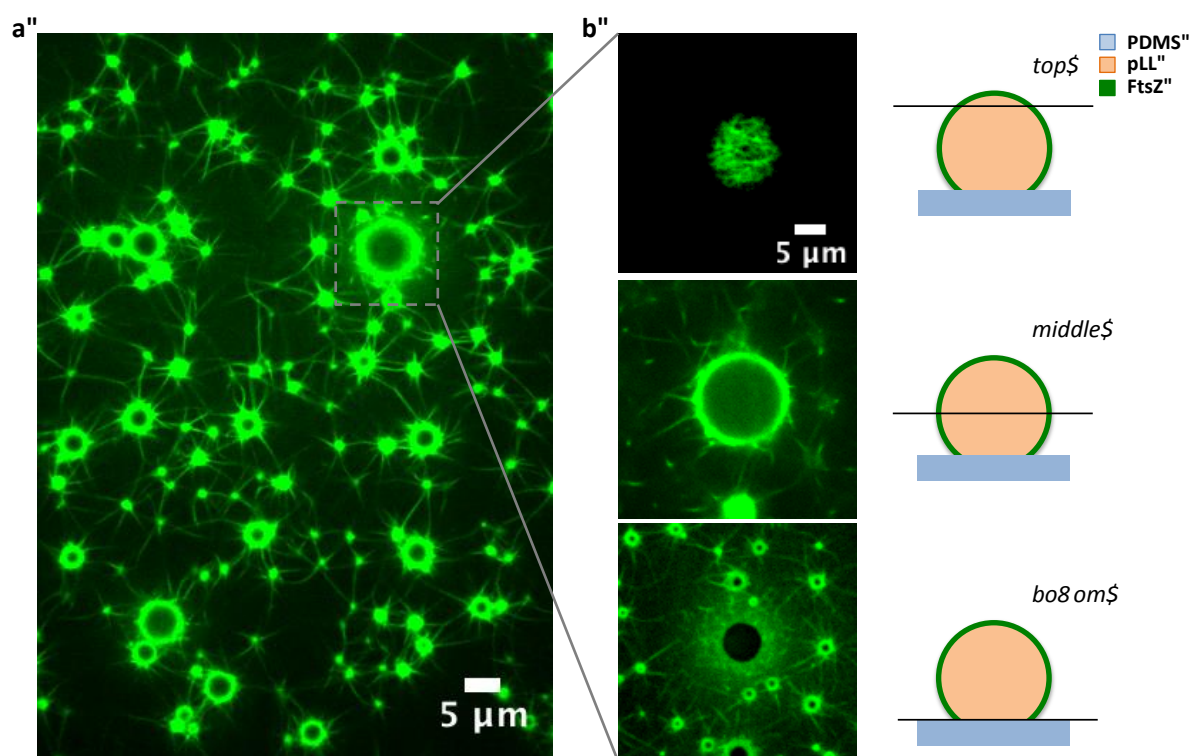
Figure 3. Localization at the coacervate surface promotes bundling of FtsZ filaments and subsequent protrusion of the bundles to form an interconnected network across multiple coacervates.

(**a**) Fluorescence image showing bundles of FtsZ filaments emanating from coacervates, giving them aster-like appearance. Bundles protruding from adjacent coacervates merged with each other to form a single, interconnected, hybrid network. (**b**) A zoom-in on a single coacervate showing three slices at different planes. The confocal scan at the top surface of the coacervate showed a dense mesh of bundles (top image). A scan across the equator showed bundles emerging out of the droplet (middle image). A scan across the bottom surface showed numerous bundles at the interface forming a dense mesh (bottom image) and dark circular regions that correspond to the area where the coacervate adhered to the surface, preventing FtsZ from gaining access.
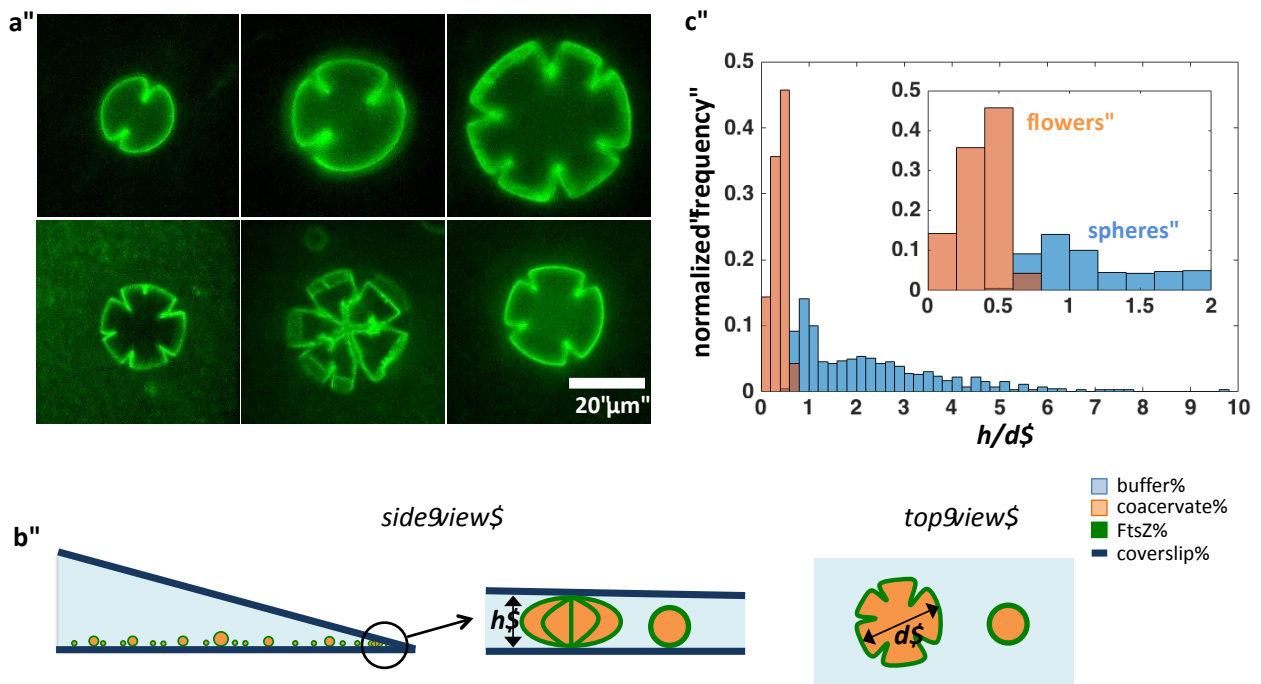
22

Figure 4. FtsZ-coated coacervates display extensive invaginations when deformed under mechanical pressure.

(**a**) Fluorescence images showing several examples of FtsZ-coated deformed coacervates, exhibiting pronounced defects in the form of multiple invaginations. We address these shapes as 'flowers'. In some cases (bottom center), invaginations divide the flower into separate petals. (**b**) A schematic showing the wedge device with a variable height that was employed to verify whether coacervates transformed into flowers only when pressed. A deformed and a non-deformed coacervate is also sketched, showing a cracked and a smooth interface respectively. (**c**) A frequency histogram (*N*=540) that shows that coacervates adopt a flower shape only when mechanically pressed, i.e., when the height *h* of the microchamber is lower than the diameter *d* of the coacervate.
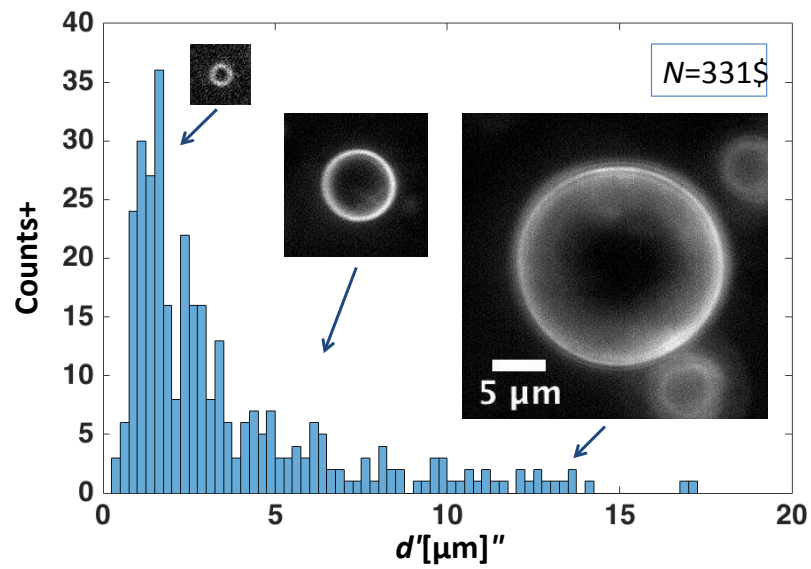
Supplementary Material

Figure S1: Size distribution of coacervates.

Frequency histogram showing a polydisperse size distribution of pLL/GTP coacervates (N = 331). As can be seen, majority of the population lies between 1−5 μm.
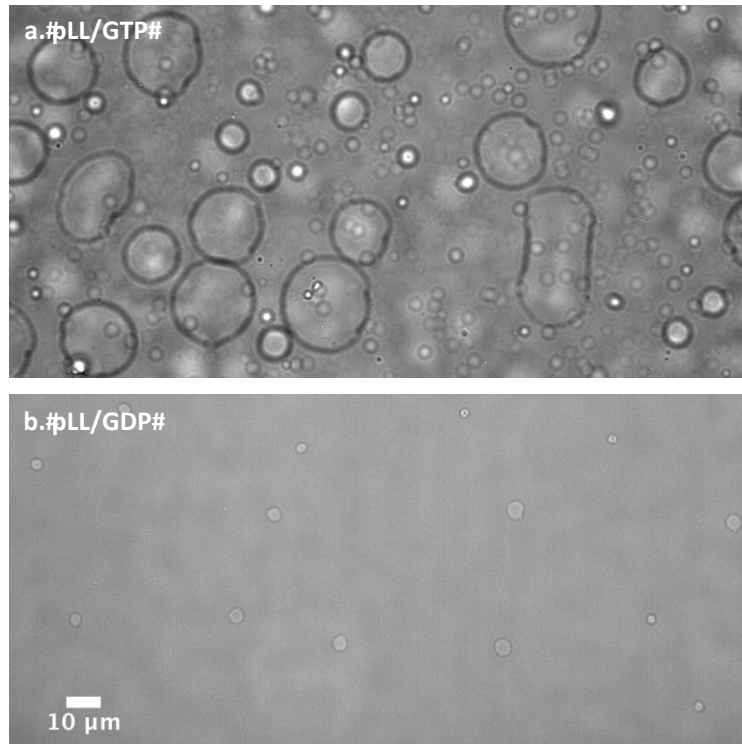
Figure S2. Coacervation efficiency is strongly influenced by the extent of multivalency of the nucleotide.

(**a**) GTP and pLL readily formed numerous coacervates when mixed together. (**b**) GDP and pLL, on the other hand, formed only a few and much smaller coacervates. The lower efficiency of the coacervation process can be attributed to the lower amount of negative charges carried by GDP molecules.
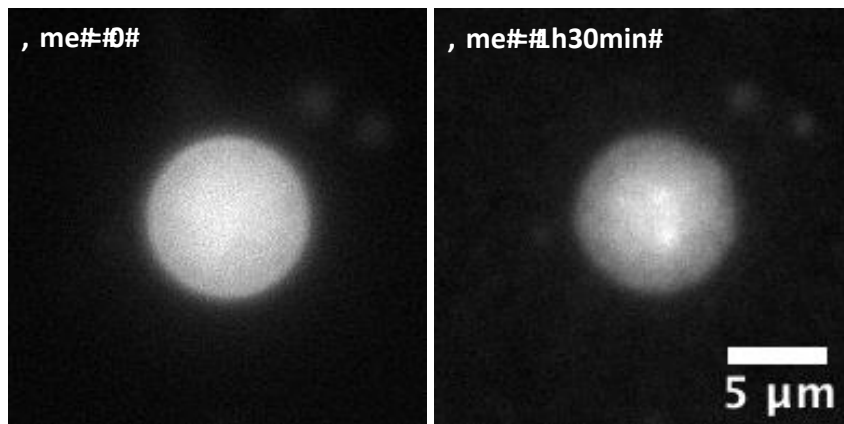
Figure S3. In absence of FtsZ, coacervates remain stable, even when flushed with a buffered solution.

When the microchamber containing the coacervates was gently flushed with a buffered solution to get rid of the excess proteins and nucleotides, the coacervates remained stable and did not change their volume.
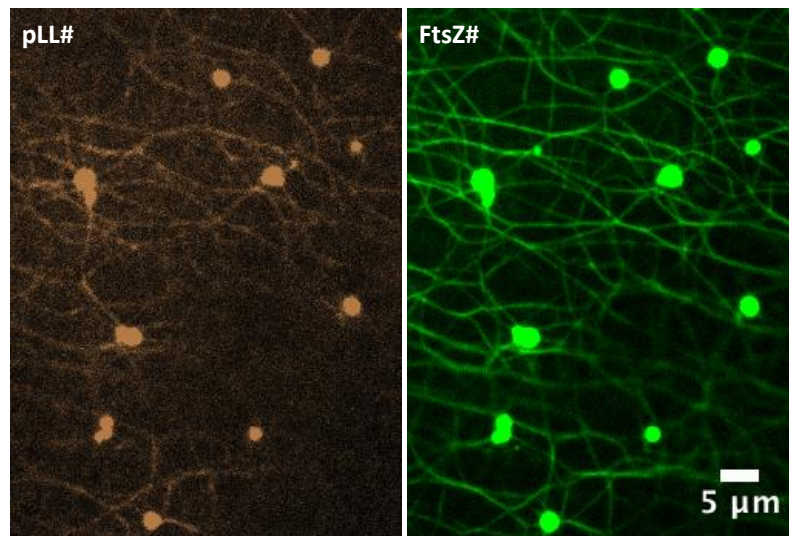
Figure S4. pLL colocalizes with the network of emanating FtsZ bundles. Incubating the coacervates with FtsZ solution for two hours and subsequently removing the proteins and the nucleotides from the surrounding solution led to the formation of thick bundles and shrinkage of coacervates. Interestingly, the fluorescent signal (false colors) from cy5-labelled pLL, colocalized with the signal from FtsZ bundles, indicating that pLL molecules interacted with, and adhered to FtsZ bundles.
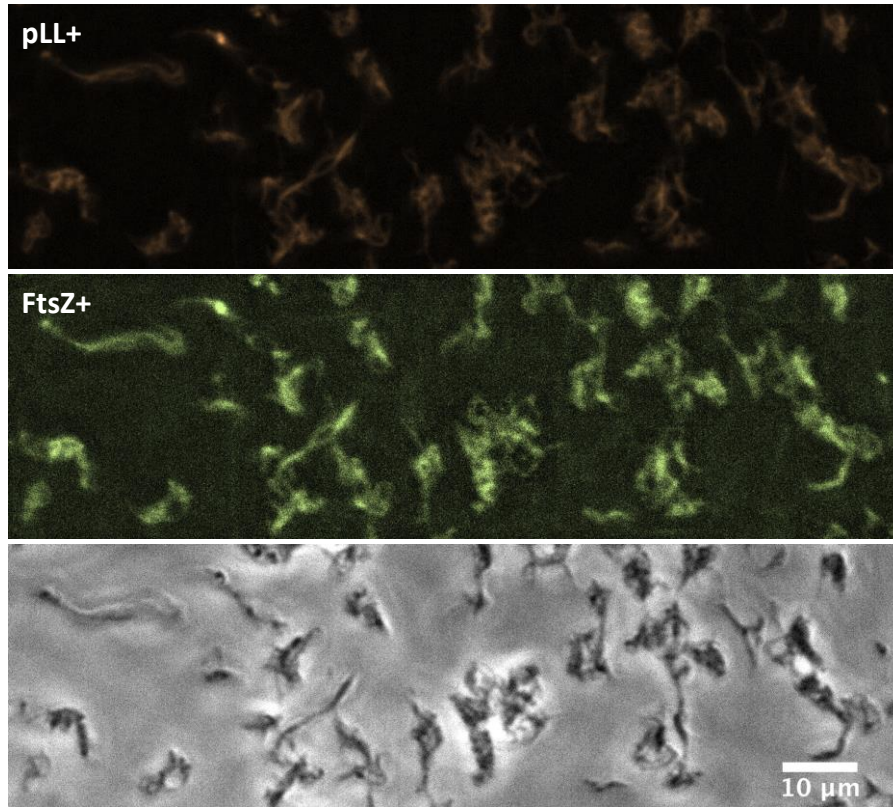
Figure S5. pLL and FtsZ interact with each other to form fiber-like structures. When mixed together, pLL (440 µM) and FtsZ (205 µM) aggregate to form filamentous structures. Co-localization is evident from overlapping of fluorescent signal of cy5-labelled pLL and Alexa488-labelled FtsZ. The images are false-coloured.
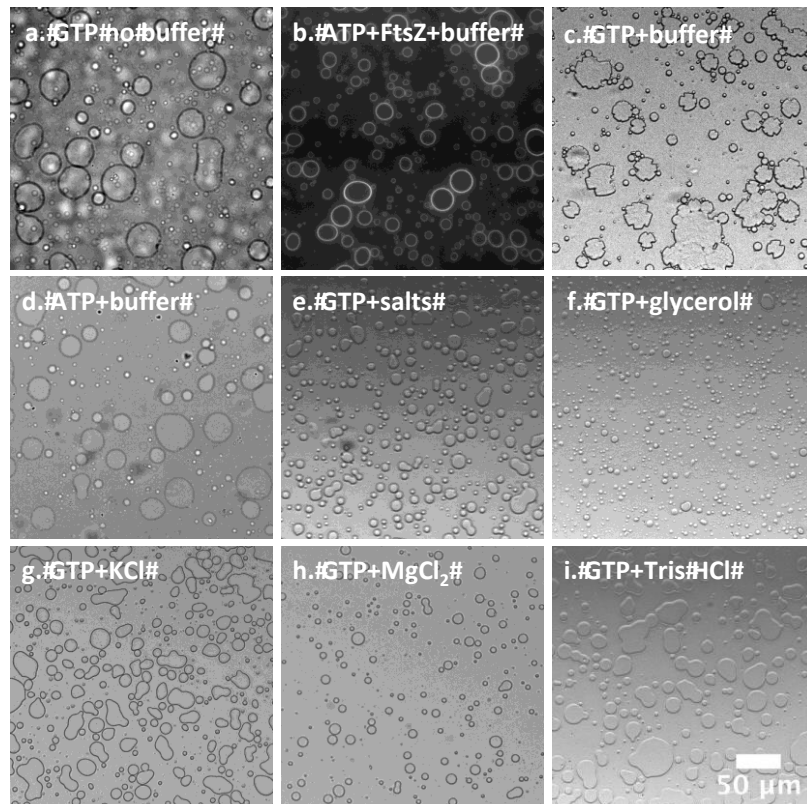
Figure S6. The morphology adopted by the coacervates under mechanical stress depends on the nucleotides base and on the buffer conditions.

(**a**) GTP/pLL coacervates did not show any invagination under mechanical stress in absence of buffer and FtsZ. (**b**) ATP/pLL coacervates covered with FtsZ did not deform into a flower-like shape. (**c**) GTP/pLL coacervates in presence of buffer showed flower-like shapes, while ATP/pLL coacervates in the same conditions did not (**d**). Without FtsZ, flower-like coacervates were not present in absence of glycerol (**e**), or when mixed only with individual buffer components, specifically 15% v/v glycerol (**f**), 150 mM KCl (**g**), 5 mM MgCl2 (**h**), 25 mM Tris HCl (**i**).